Journal of Applied Fluid Mechanics, Vol. 17, No. 4, pp. 926-938, 2024.
Available online at www.jafmonline.net, ISSN 1735-3572, EISSN 1735-3645.
https://doi.org/10.47176/jafm.17.4.1900

Flow Modeling in the Wake of a Francis Turbine with Hydraulic Charge: Case of Songloulou-Cameroon

R. D. Wafo [1†], M. Tientcheu-Nsiewe [2], D. Tcheukam-Toko [3], B. Kenmeugne [4] and A. Kuitche [5]

[1] *Department of Mechanical engineering, National School of Agro-Industrial Sciences, University of Ngaoundere, Cameroon*
[2] *Department of Fundamental Sciences and Engineering Technics, School of Chemical Engineering and Mineral Industry, University of Ngaoundere, Cameroon*
[3] *College of Technology, Department of Mechanical Engineering, University of Buea, Cameroon*
[4] *Department of Mechanical engineering, National Higher School Polytechnics of the University of Yaoundé, Cameroon*
[5] *Department of Energetics, Electric and Automatics engineering, National School of Agro-Industrial Sciences, University of Ngaoundere, Cameroon*

† *Corresponding Author Email: raoul.wafo@univ-dere.cm*

ABSTRACT

Cavitation in hydraulic installations is still a major concern when it comes to producing electricity. We are aware of the danger of cavitation and the damage it can cause. We have carried out a study of the behavior of the Francis de song lou lou turbines in operation, their areas of application and their various modes of degradation. The first step was to identify the nature of cavitation during operation. We used the three-dimensional Naviers Stokes equations. The pressure and velocity fields obtained are examined to observe the various fluctuations that disrupt the correct operation of the turbine, and consequently reduce production efficiency. The characteristics of the turbine at the Song Loulou hydroelectric power station in Cameroon were used. The results obtained, compared with those in the literature, are satisfactory. This modelling is an effective tool for detecting the presence of cavitation in the Francis turbine.

Article History

Received April 7, 2023
Revised November 24, 2023
Accepted November 25, 2023
Available online January 30, 2024

Keywords:

Instabilities
Blades
Francis Turbine
Numerical Modeling
Hydraulic charge

1. INTRODUCTION

Hydraulic turbines are the central element of hydroelectric production. The purpose of this study is to detect the presence of cavitation in the Francis turbine wheel at the Song loulou hydroelectric power station in cameroon. Turbine operating stability is generally satisfactory for nominal operating conditions. However, outside the rated speed, hydraulic machines with fixed blades such as Francis turbines very often induce dynamic instabilities linked to the inevitable vorticity at the wheel outlet. The demands of today's technology mean that we can build machines that are ever more advanced, and therefore more exposed to disturbed regimes. Depending on the operating conditions of the installation, these excitations may be barely perceptible, bearable or even unacceptable (Gino, 2000). Cavitation is a crucial problem facing designers and users of hydraulic machines.

The development of cavitation at the blade inlet of a hydraulic machine is often the cause of severe erosion, which can lead to the premature shutdown of the machine, with considerable economic consequences (production stoppage, maintenance costs, etc.). Erosion occurs when steam cavities are convected into areas of pressure above the saturation steam pressure. If they implode close to the walls, there is a significant risk that shock waves will attack the material (Max, 2011). Cavitation, which develops in a hydraulic turbine, is also accompanied by a drop in performance, the generation of vibrations in the mechanical structure and a disturbing noise emission. Aware of the danger represented by the development of cavitation and the damage that can result, manufacturers and users of hydraulic machines insist on the level of installation of their machines and the adaptation of the angles of incidence of the flow on the blades. They contribute to surface damage and installation instability through excessive vibration. The fields concerned by this problem cover a very wide range of industrial applications. In particular, hydroelectric infrastructure (dam discharge channels), shipbuilding (marine propellers) and power generation (turbines) (Nicolet & Avellan, 2002). Cavitation damage has always been a serious problem of technical instability.

More specifically, we are interested in the cavitation phenomenon encountered in the Francis turbine wheel at

Nomenclature

H	distance separating one of the two holes and the main axis	ε	turbulent kinetic energy dissipation rate
P	pressure	k	turbulent kinetic energy
T	temperature difference	ρ	density
ΔT_{ref}	temperature difference between the hot jet and the outside	0y	vertical axis
0x	longitudinal axis	0z	transverse axis

the Song Loulou hydroelectric power station, and will investigate the causes of cavitation and the various disturbances resulting from it. It will therefore be important to carry out an analytical study of the dynamic velocity and pressure fields in the Francis wheel, and to make a comparison with studies in the literature in order to observe its behaviour in operation. The numerical tools at our disposal will be used to detect the presence of cavitation in the Francis turbine wheel at Song Loulou and to identify the type of cavitation by comparison with studies in the literature.

2. STATE OF THE ART

Research in the field of cavitation is mainly directed towards the prediction and prevention of hydraulic instabilities. The prediction of the instability is an extremely difficult problem, the possible problems are noted only with the setting in service of the industrial installation; yield losses cause considerable damage to both the operator and the builder. It can be seen that the flow at the wheel inlet is characterized by eddies (Ciocan et al., 2015). The wake is studied, and the non-uniformity of the flow is observed, thanks to numerical studies in addition to experimental studies. The inlet flow is influenced by the vortices, right up to the impeller outlet (Mauri, 2002). The strong pressure gradients coupled with the shape of the blades create the separation of the boundary layers (Duprat et al. 2009).

Regarding digital studies, the CFD is used to carry out an assessment of the performance of hydraulic turbines (Gyanendra & Kumar, 2020). The flow regime infections on the drop in yield of Francis turbines (Arn, 1998). The case of an isolated bubble is treated by Ceccio et al. (1995). They provide a detailed description of the behavior of the converted bubble on hydrodynamic profiles. Due to its geometry, the bubble rarely retains its spherical appearance, even if it seems to have a circular base, the height of its interface is larger in the upstream part. Observations also reveal a complex flow around the bubble. The movement of the latter, generates local turbulence areas crossing an unstable limit layer. An energy approach is proposed to develop a model for predicting cavitation erosions (Pereira, 1997). Based on the knowledge of the energy spectrum associated with the development of an attack edge cavitation pocket, it is established on the basis of the measurement and analysis of three main quantities: the volume of the transitional cavities, the Motor pressure of implosion and the rate of production of cavities (Blommaert, 1995). The use of vibration or acoustic detection methods of cavitation is also proposed to prevail absolute information on the erosion rate and the cumulative loss of metal (Ding et al., 2021; Bourdon, 2000). The technique consists in measuring the vibrations induced on the fixed parts of the turbine, and of extracting the contribution of the impact of cavitation on the blades. Maged (2003) supposes that the rate of loss of matter varies depending on time. He suggests that, the weight loss by weight of the material can be represented by a distribution of Weibull with two parameters. The author concludes that, according to all the results obtained in the laboratory, the Weibull model remains plausible, but depend on the different parameters of the material used, the incubation time and the duration of the tests. Pallegrino and Meskell (2013) Use vortex detachment on a section of the blade to analyze cavitation attacks around the blade in order to understand its behavior. In the same approach, (Monica et al. 2009), an experimental analysis of the cavitation whirlwind in the vacuum cleaner of a Francis turbine is made in order to determine the influence of the speed and shape of the rope on the instability of the turbine on A reduced model. The result shows the displacement of the cavitation vortex for the value of the cavitation number equal to 1.180 and 0.380. The greater the number of cavitation, the greater the vortex.

In order to determine the pressure fluctuations (Jacob & Married 1988) made an experimental study of the dynamic behavior of a Francis turbine at high load. They made comparisons on the model-prototype. They determine the pressure fluctuations, and demonstrate the presence of high load torch instability, which causes mechanical and electrical oscillations. The results show the peaks observed on the amplitude spectrum of the pressure oscillations, this recorded at high load in the cone of the aspirator of the scale model of the Francis turbine. Which corresponds to natural frequencies of the hydraulic system. The harmonic response curve and spectrum recorded under excitation on the Fraude drop are presented in Fig. 1, together with the amplitude frequency comparison curve and external excitation as a function of the natural frequency calculated from observations of flare volumes.

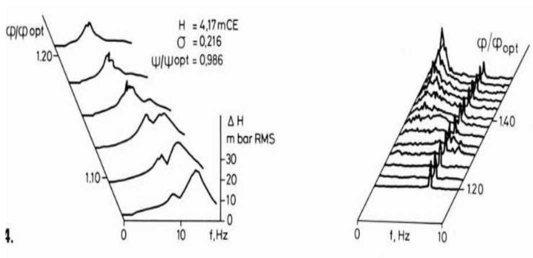

Fig. 1 harmonic response curve and spectrum measured without excitation (Jacob & Married 1988).

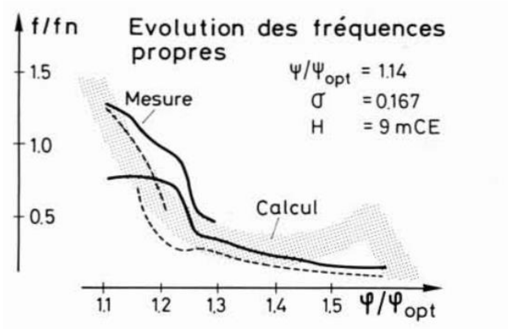

Fig. 2 Comparison curves of amplitude frequencies and external excitation.

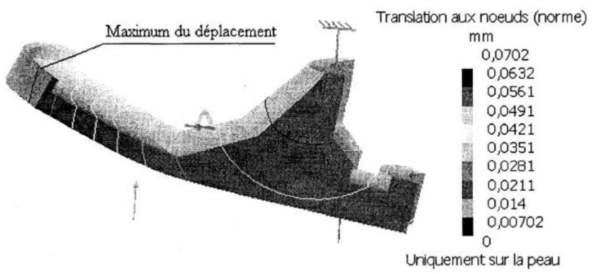

Fig. 3 result of displacement of the simplified blade top seal at a pressure of 5 10^5 N/m^2

The cavitation flare in Francis-type hydraulic turbines was modeled by Goulet (1999). He uses the FIDAP software to observe areas of depression and high vorticity. It is in this logic that, Alca (2003) performs an analysis of the pressure field on the wall of the diffuser of a Francis turbine, in order to bring out the fluctuating fields which propagate from the wheel to the elbow outlet. It makes measurements at the operating points of the partial flow. (Khalfi, 2005) contributed to the development of a code for calculating the stresses in a Francis turbine. It defines the simple geometric model of the ceiling, represents the pressure field and simulates the structure. The results are shown in Fig. 3.

This result allows designers to have an idea of the nature of the stresses in the ceiling vane joint. (Monica et al., 2009), propose an experimental and numerical study of the vortex vortex in the diffuser of a Francis turbine to determine the dynamic conditions of the cavitation vortex, in order to make a comparison of the simulation with the results obtained by experimentation. (Xiaa & Zongguo, 2010) makes a numerical analysis of an unstable flow under high pressure operating conditions in a Francis turbine. His results show pressure peaks inside the wheel, which causes an imbalance in operation. Ciocan et al. (2015) carries out a numerical study of cavitation detection in a prototype of the Francis turbine, they show through the curves, the fluctuation of pressures in the Francis wheel which is the cause of the disturbances in operation. Part load transient pressure measurements of a Francis turbine, high load model, Detailed analysis showed vortex degradation of rotating components. (Xavier & Egusquiza, 2006) simulates the flow of a cavitating flow vortex cable in a Francis turbine, at part load conditions

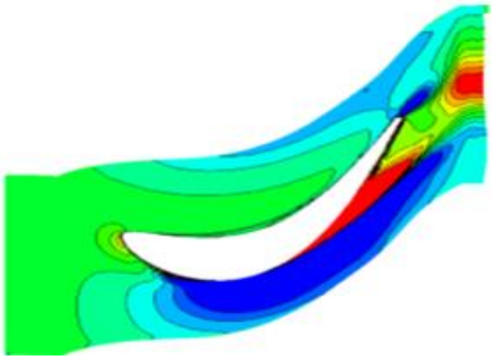

Fig. 4 Pressure distribution on the blade (Houde et al., 2014)

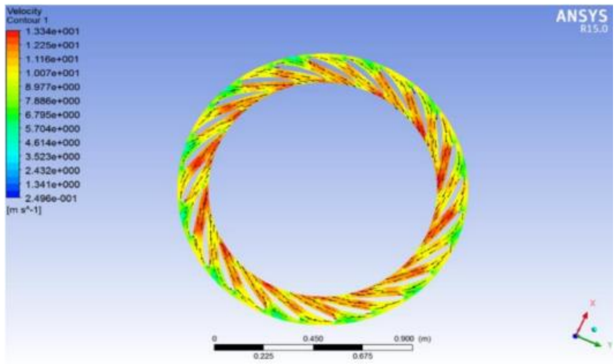

Fig. 5 variation of the velocity field in the spiral cover and at the entrance to the wheel

for different levels of σ. It compares pressure fluctuations for different levels of σ with experimental data . It shows that, for σ =0.09, the maximum pressure amplitude is 0.12; for σ =0.11 the maximum pressure amplitude is 0.15. The closer the cavitation coefficient is to 0, the lower the cavitation. (Wahidullah & Vishnu, 2016) modeled the impact of turbulence and fluid physical properties on the blade of a Francis turbine. The turbulent flow distribution is shown in Fig. 4.

A zone of high pressure and a zone of low pressure localized at the level of the upper surface of the blade are observed. The variation of the hydraulic head in the Francis turbine creates instabilities in the runner. It appears from works of (Houde et al., 2014), after a numerical study on CFD, The spiral cover shows a continuous flow in each section of the distributor, the flow velocity increases when approaching the turbine and the pressure variation has areas of high and low pressure all around the Francis wheel.

The pressure distribution in the runner of a Francis turbine (Saeed & Popov, 2012), clearly shows the gradual reduction in high pressure. It goes from the spiral cover to the turbine, and a low pressure is observed at the outlet of the wheel. A large water pressure is observed at the leading edge of the wheel, and the pressure drop on the blades. It results from the rapid decrease in the amplitude of the tangential velocity in the flow: this is the phenomenon of cavitation.

The work of (Jing & Liu, 2021), deals with the analysis of the pressure at the outlet of the Francis turbine wheel under stable and transient conditions. The high cavitation zone represents the low-pressure zone, this low-pressure zone then forms a cavitation flare which originated in the turbine. (Wahidullah & Vishnu, 2017), make a numerical study of the cavitation in a Francis turbine of a small hydroelectric power station. The results present the variation of the pressure in the Francis turbine.

The pressure variation at part load, nominal load and overload conditions are obtained in the figure above. It has been found that, the pressure decreases from the inlet of the impeller towards the outlet of the diffuser. And the speed increases from the entry towards the exit of the wheel according to the variation of the pressure. However, the pressure difference was found in the overload condition, as compared to the nominal load condition. Low pressure is observed on the vacuum side of the trailing edge under an overload condition. At the leading-edge, low-pressure values are also observed under nominal load conditions. The behavior of pressure fluctuations or pulsations is an important feature to understand the presence of instabilities.

3. MATERIALS AND METHODS

3.1 Geometric Modeling

Each component is modeled separately and then assembled via appropriate interfaces. A simulation analysis is performed for the Francis turbine, the rotational speed of the runner is specified. The accuracy of any CFD analysis is highly dependent on the boundary conditions, which must be specified at different boundaries of the flow domain. If the boundary conditions are not used correctly for the definition of the physical problem, the solution can be completely erroneous (Zhumei & Nie, 2022). Boundary conditions influence the direction of the flow, the fluxes of mass, energy and momentum. It is quite possible that different boundary condition data items produce different simulation results (Eric and Elcilane, 2022). The water flow rate in the Francis turbine and the flow direction are specified at the turbine inlet as the boundary condition. Pressure and velocity are specified as the impeller outlet boundary condition.

In the current case, the flow is 135.7 m³/s. The guide vane opening is 70.93 mm, the full guide vane opening is 107.6 mm. The reference pressure is taken as equal to 1 atmosphere or 10 5 Pa. The speed of rotation of the wheel is specified at 120 rpm according to the opening of the guide vanes; the domains are considered stationary. Shear stress transport (SST), k-ε is the turbulence model used and the walls of all domains are assumed to be smooth without slippage. Figure 6 shows the geometry of the Francis wheel and the spiral blanket in our study.

3.2 Mathematical Formulations

Computer analysis provides pressure and velocity distribution over the entire turbine region in the form of pressure and velocity profile. Losses in various domains

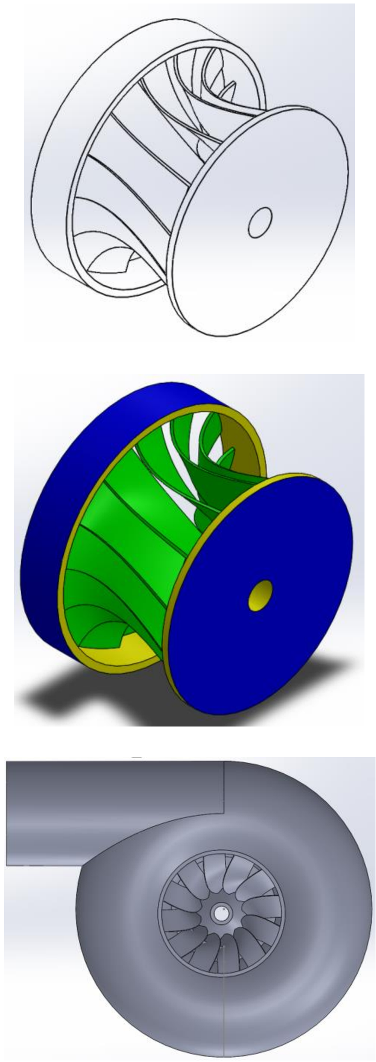

a)

b)

c)

Fig. 6 a)- b)- c) Physical model of the Francis turbine wheel and spiral cover.

are calculated based on the pressure difference, and at the inlet and outlet boundary of the study domain. Various formulas are used for the calculation of the different parameters.

To characterize the appropriate type of Francis runner, the notion of specific speed is introduced, which forms the basis of the characteristics and classification of turbines. As the specific speed increases, the shape of the impeller vanes gradually changes from radial to axial.

Specific speed: $N_S = N\frac{\sqrt{P}}{H^{\frac{5}{4}}}$ (1)

Power available: $P = \rho g Q H$ (2)

Pressure: $P_r = \rho g H$ (3)

The static pressure at the inlet of a Francis turbine is generally well known, based on the change in vertical elevation from the inlet of the turbine to the free surface of the water feeding the turbine. For these reasons, a full pressure condition will be used as the entry condition. The total pressure is specified as the inlet boundary condition as given by equation 1.

$$P_{t1} = P_1 + \frac{1}{2}\rho\left(\frac{Q}{A_1}\right)^2 \quad (4)$$

The static pressure applied to the downstream boundary using Bernoulli's principle as shown in equation 2. Let 1 at the inlet and 2 at the outlet:

$$P_2 = P_1 + \rho\left[\frac{Q^2}{2}\left(\frac{1}{A_1^2} - \frac{1}{A_2^2}\right) + g(z_1 - z_2)\right] \quad (5)$$

The Navier Stokes average momentum conservation equations known as RANS, are for an incompressible fluid and Newtonian name given by the following formula:

$$\frac{\partial U_i}{\partial X_i} = 0 \quad (6)$$

$$U_j\frac{\partial U_i}{\partial U_j} + \frac{1}{\rho}\frac{\partial P}{\partial X_i} - \frac{\partial}{\partial X_i}\left(\nu\left(\frac{\partial U_i}{\partial X_j} + \frac{\partial U_j}{\partial X_i}\right) - \tau_{ij}\right) = 0 \quad (7)$$

Where U, P, ν, and ρ are the velocity, pressure, kinematic viscosity, and density, respectively, and τ_{ij} is the component of the viscous stress tensor, also called the Reynolds stress tensor. The turbulent effects on the flow field are through the Reynolds stresses τ_{ij}, which were calculated from the k-ε turbulence model adopted in this article for its better numerical convergence and robustness. The governing equations are discrete with finite volume method, and the diffusion item, and the second-order upwind format is used for the convection item, and the Semi-Implicit Method for Pressure-linked Equations-consistent (SIMPLEC)

The set of transport equations for the feasible k-ε model are:

The turbulent kinetic energy equation is given by the following formula:

$$\frac{\partial}{\partial t}(\rho k) + \frac{\partial}{\partial x_i}(\rho k u_j) = \frac{\partial}{\partial x_i}\left[\left(\mu + \frac{\mu_t}{\sigma_k}\right)\frac{\partial k}{\partial x_j}\right] + G_k + G_b - \rho\varepsilon - Y_M \quad (9)$$

And the equation for the rate of dissipation of turbulent kinetic energy by:

$$\frac{\partial}{\partial t}(\rho\varepsilon) + \frac{\partial}{\partial x_j}(\rho\varepsilon u_j) = \frac{\partial}{\partial x_j}\left[\left(\mu + \frac{\mu_t}{\sigma_\varepsilon}\right)\frac{\partial \varepsilon}{\partial x_j}\right] + \rho C_1 S\varepsilon - \rho C_2\frac{\varepsilon^2}{k+\sqrt{\upsilon\varepsilon}} + C_{1\varepsilon}\frac{\varepsilon}{k}C_{3\varepsilon} \quad (10)$$

3.3 Computational Flow Parameters

Methodology of work

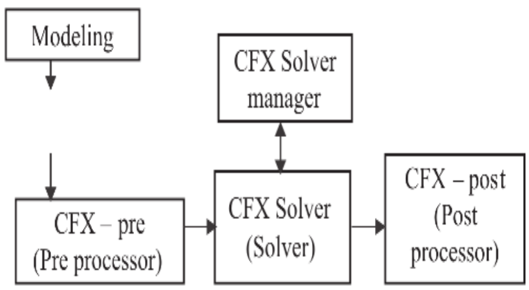

Fig. 7 Algorithme de validation des résultats

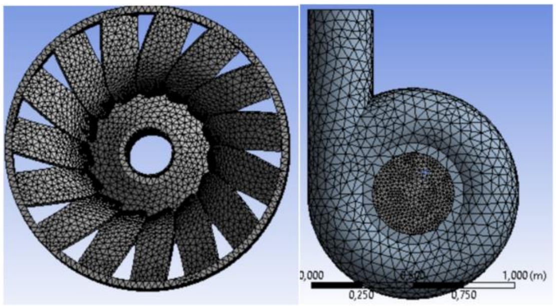

(a) (b)

Fig. 8 Wheel and diffuser mesh

Table 1 Summary of mesh

Domain share	No. of nodes	N° of elements
Casing	150,427	236,415
runner	87.974	48,251
draft tube	98,485	75,228

4. RESULTS AND DISCUSSION

The unstructured tetrahedral mesh is generated for all areas of the study. The accuracy of the solution is strongly influenced by the size of the elements (Bousquet et al., 2016). The Francis turbine consists of 15 blades and a spiral blanket. The mesh of the Francis turbine wheel and spiral cover is shown in Fig. 8.

4.1 Model Validation

The observation made in Fig. 14 shows the variation of the pressure field in the spiral cover of the Song Loulou Francis turbine. The high pressure at the inlet of the spiral cover decreases as one approaches the turbine. The pressure drops considerably in the turbine and is observed at the outlet of the turbine. This pressure drop in the turbine is proof of the presence of cavitation in the Song Loulou Francis turbine.

The comparison of the results of the work of (Saeed & Popov, 2012), and our study, shows a uniformity of:

- the pressure distribution in the spiral cover of the Francis turbine.
- The high pressure zone is observed at the entrance to the spiral cover.
- The pressure drop observed in the different Francis turbines.

These phenomena clearly show the same pressure variations and the same pressure parameters inside the turbine, it is the presence of cavitation.

4.2 Study of the Pressure Field in the Spiral Cover

The different static and dynamic pressure fields in the spiral cover of the Song Loulou Francise turbine are examined. This allows us a good observation of the flow behavior on the orthogonal, longitudinal and transverse plane of each section of the tank.

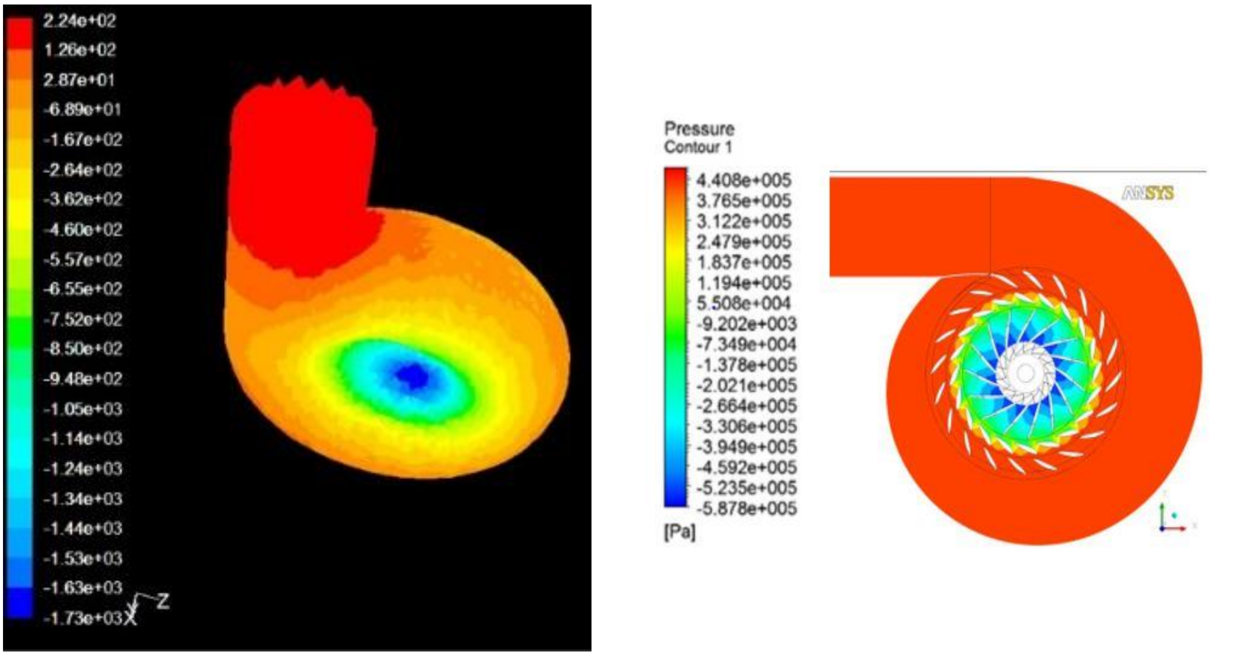

a) b)

Fig. 9 a) pressure fields in the spiral head of the Francis turbine of the Song loulou power plant, b) pressure distribution around the Francis turbine of the Derbendikan hydropower plant (Saeed & Popov et al. 2012).

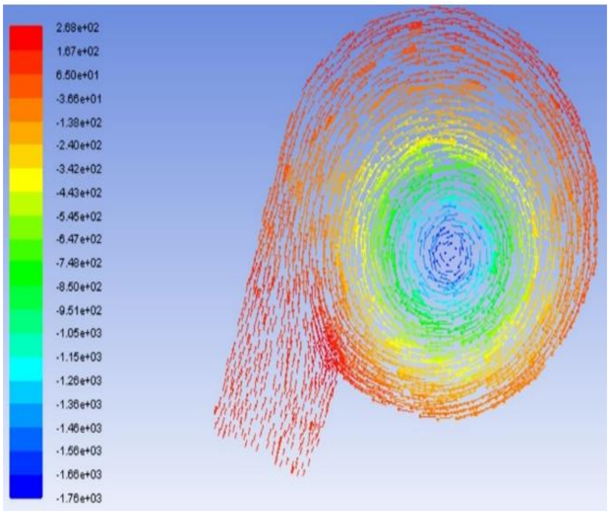

X^{+}= 0,2

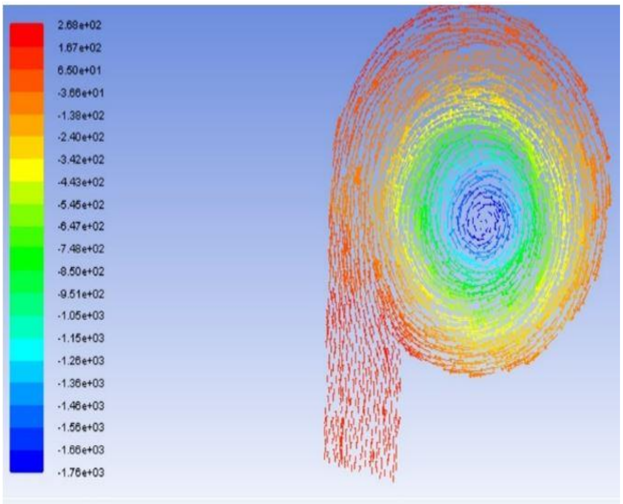

X^{+}= 0,4

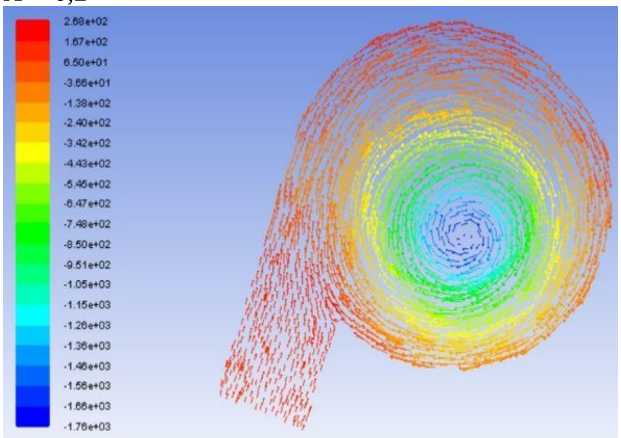

X^{+}= 0,6

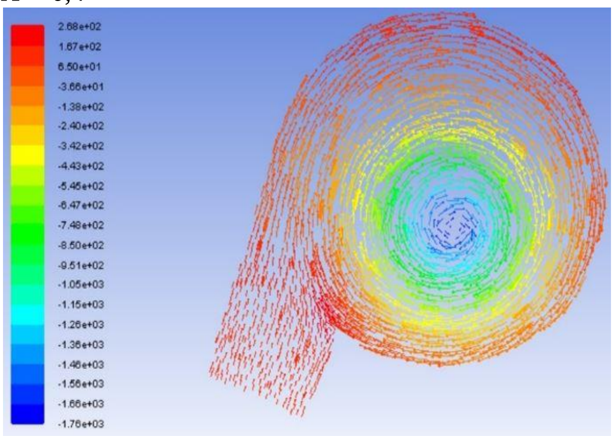

X^{+}= 0,8

Fig. 10 Static pressure field along the orthogonal plane

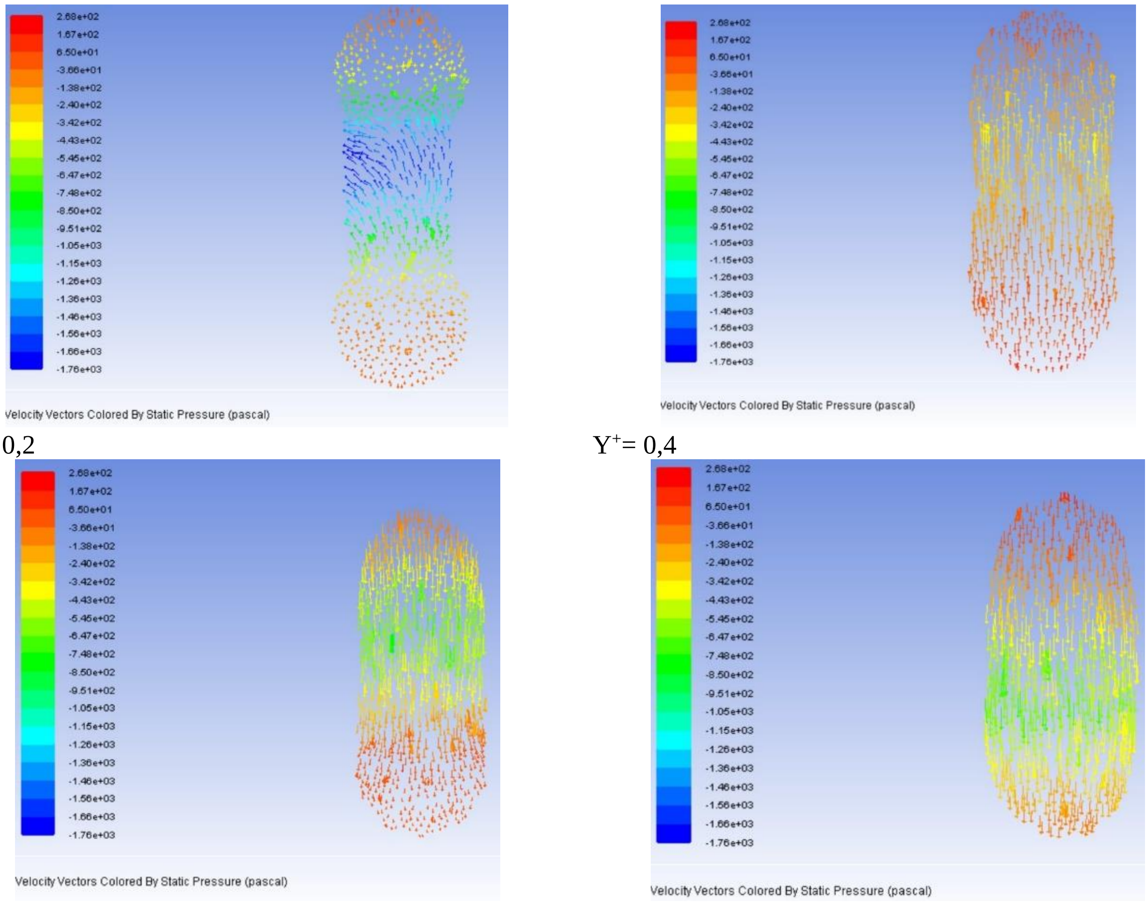

Y^{+}= 0,2 Y^{+}= 0,4

Y^{+}= 0,6 Y^{+}= 0,8

Fig. 11 Static pressure field along the transverse plane

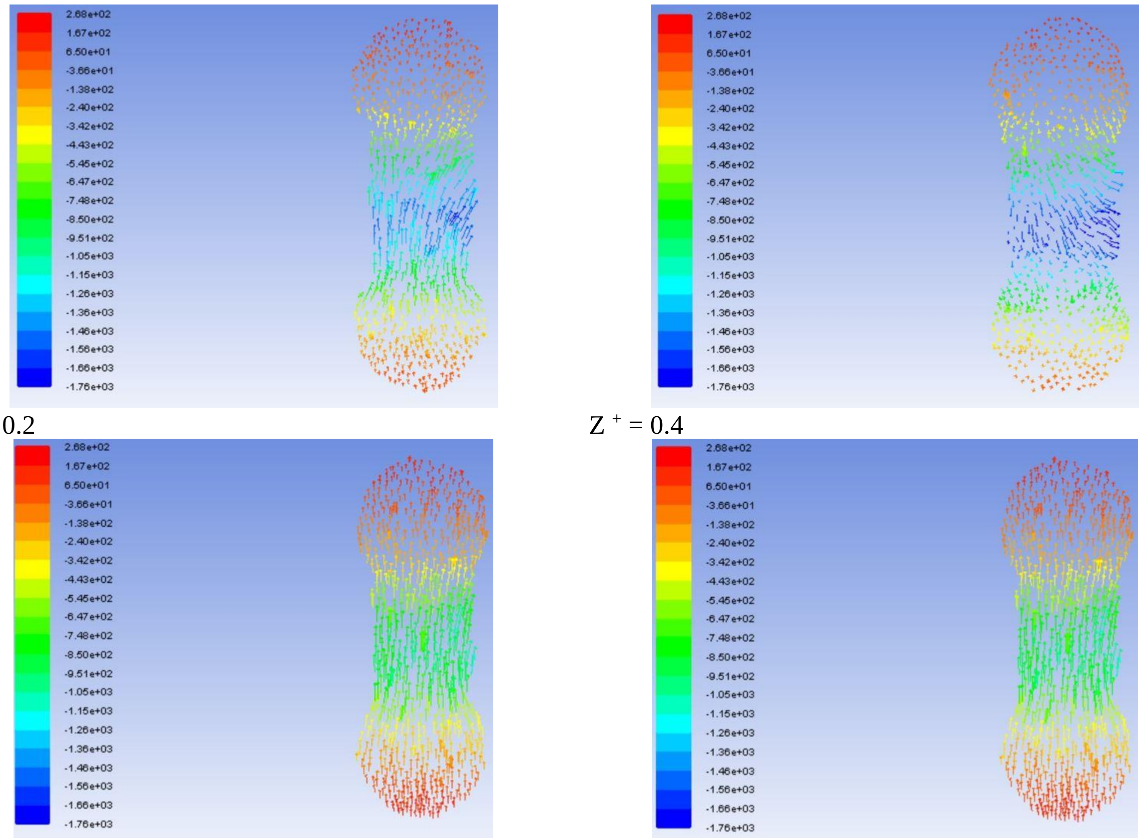

Z^{+}= 0.2 Z^{+} = 0.4

Z^{+} = 0.6 Z^{+} = 0.8

Fig. 12 Static pressure field along the longitudinal plane

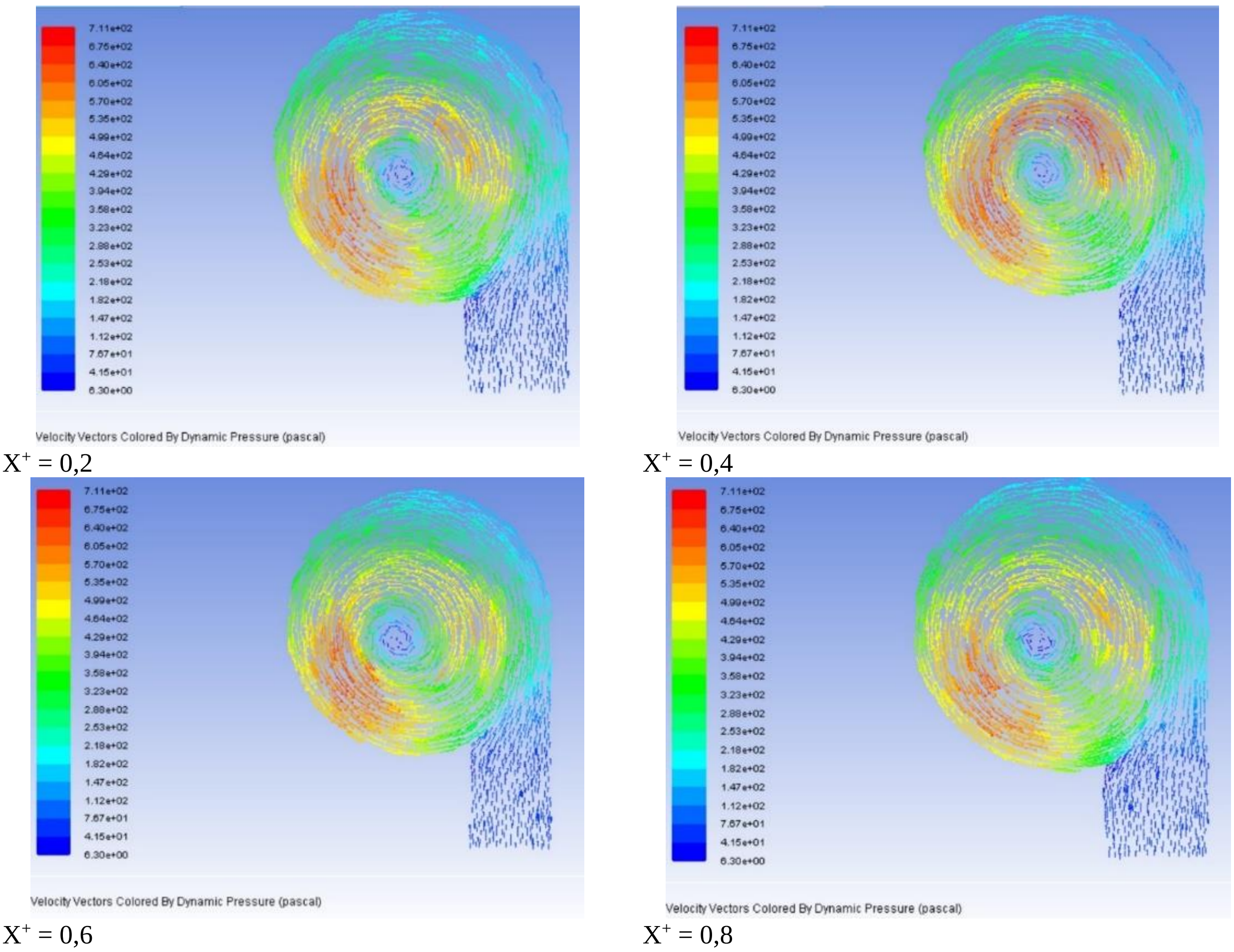

Fig. 13 dynamic pressure fields along the orthogonal plane

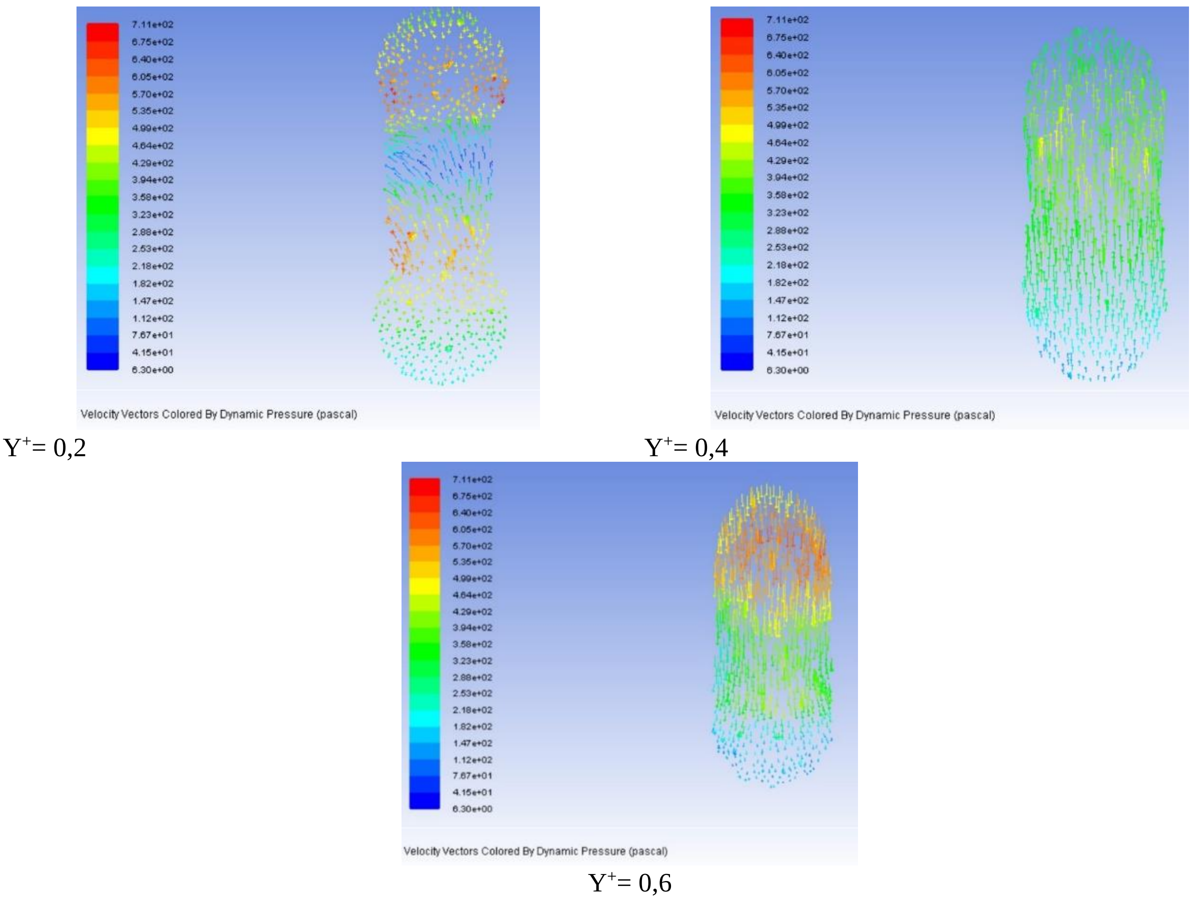

Fig. 14 dynamic pressure fields along the transverse plane

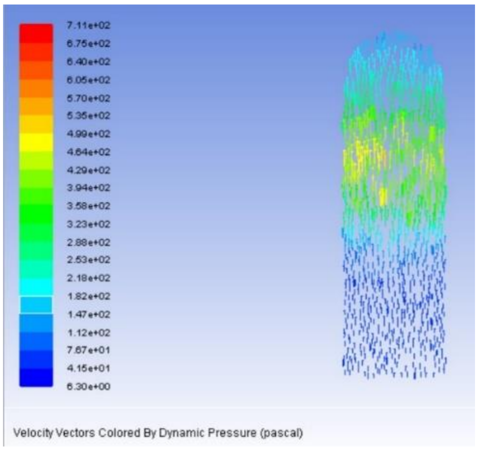

$Z^+ = 0.2$

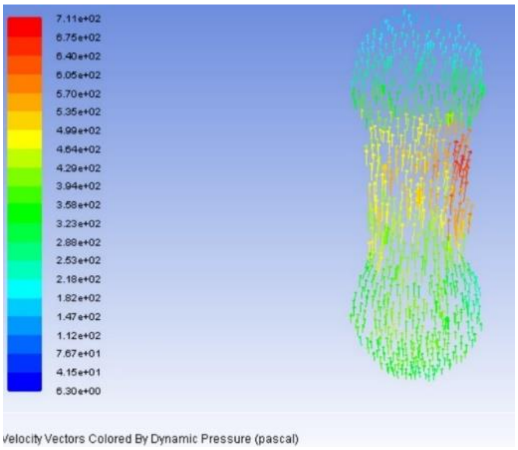

$Z^+ = 0.4$

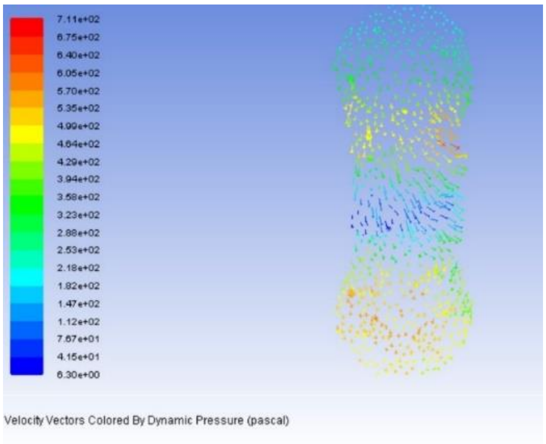

$Z^+ = 0.6$

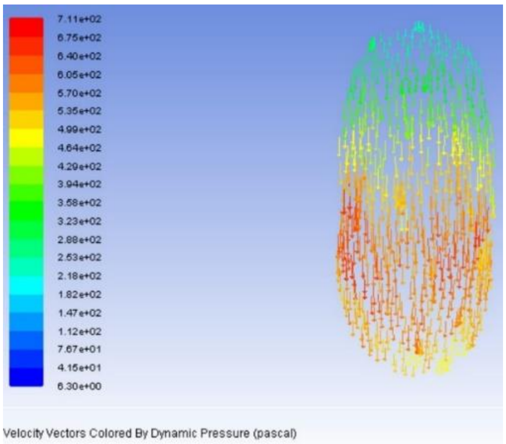

$Z^+ = 0.8$

Fig. 15 dynamic pressure fields along the longitudinal plane

a- Static Pressure Fields

We observe here, a flow is perfectly symmetrical on both sides of the axis of the diffuser. This creates a uniform distribution of velocities during the flow. The static pressure decreases as one approaches the turbine. which shows a perfect flow in the turbine.

b- Dynamic Pressure Fields

The flow is perfectly symmetrical on either side of the axis of the diffuser. The dynamic pressure increases as one approaches the turbine.

The comparison made between the dynamic pressure and the static pressure in the turbine is that the dynamic pressure increases as one approaches the turbine, then drops considerably inside it; as the static pressure gradually decreases to the turbine inlet. This comparison allows us to understand that the dynamic pressure perfectly characterizes the turbulent flow inside the turbine.

It is observed globally that the flow in the spiral cover is perfectly uniform on all planes. The static pressure effectively decreases on all of its surfaces as it moves towards the turbine. While the dynamic pressure increases towards the turbine and drops in the turbine, in the figure, we observe the different pressures on both sides of the spiral cover and these pressure variations are evenly distributed.

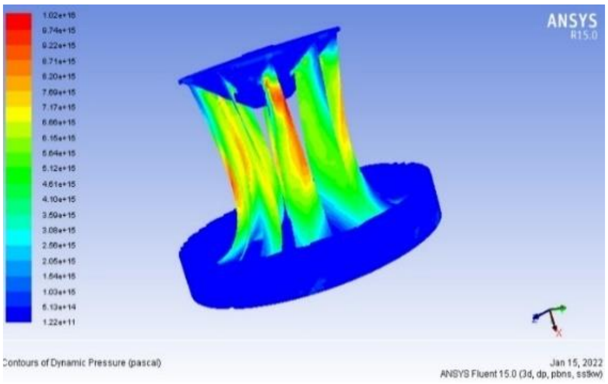

a)

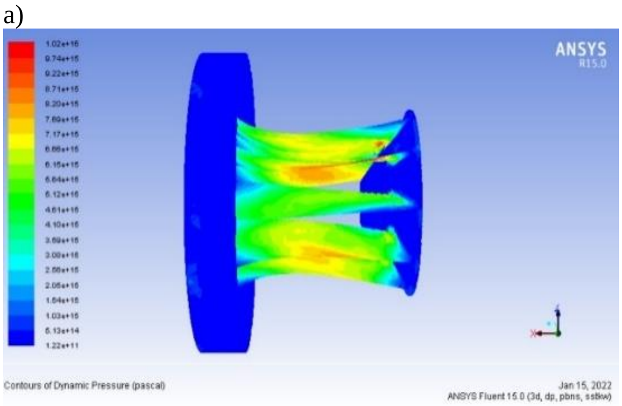

b)

Fig. 16 Dynamic pressure field in the Francis turbine runner

4.3 Study of the Pressure Field in the Wheel of the Francis Turbine at Song Loulou

There is a pressure drop at the level of the extrados of the turbine caused by the turbulence of the water flow and the presence of steam bubbles in the turbine; Pressure is disproportionately distributed around the blades due to hydraulic head which may be too low or too high This explains a localized pressure variation inside the wheel and causes the presence of instabilities in the Francis wheel characterized by cavitation phenomena.

The comparison of the pressure fields in the Francis wheel of Songloulou with the work of (Gohil & Saini, 2016) shows the areas of low pressure at the leading edge located on the upper surface of the blade; The pressure is strong at the inlet of the turbine then, it drops considerably at the outlet of the turbine which causes the presence of instabilities in the Francis wheel characterized by the phenomena of cavitation.

4.4 Modeling Turbulence in the Wheel of the Francis Turbine

The modeling done in the wheel of the Francis turbine aims to observe the behavior of the flow and the distribution of the pressure between the blades.

The flow velocity in the diffuser increases as it approaches the impeller, at the level of the blades, the contact shocks cause the birth of a cavitation flare and causes irregular turbulence around the blades.

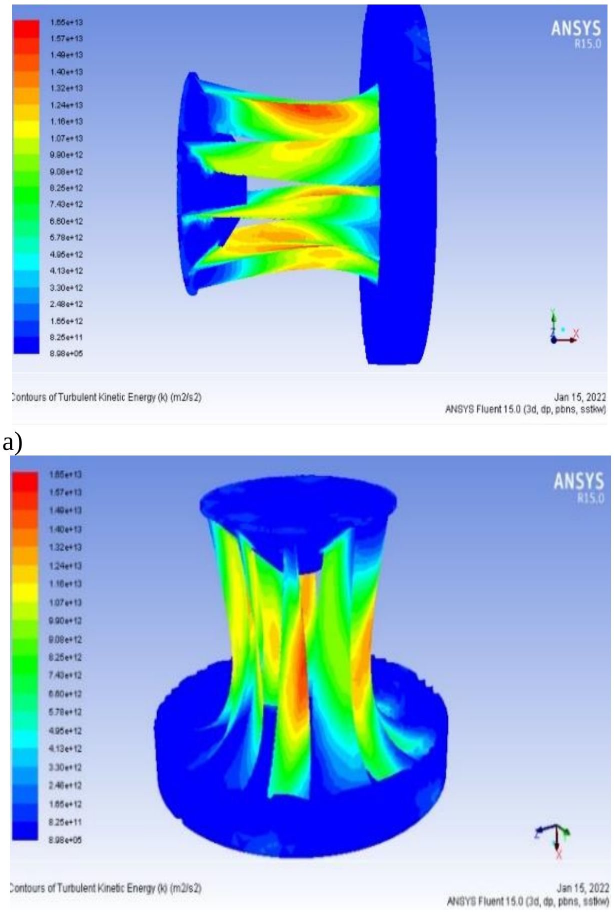

a)

b)

Fig. 17 Turbulent kinetic energy k

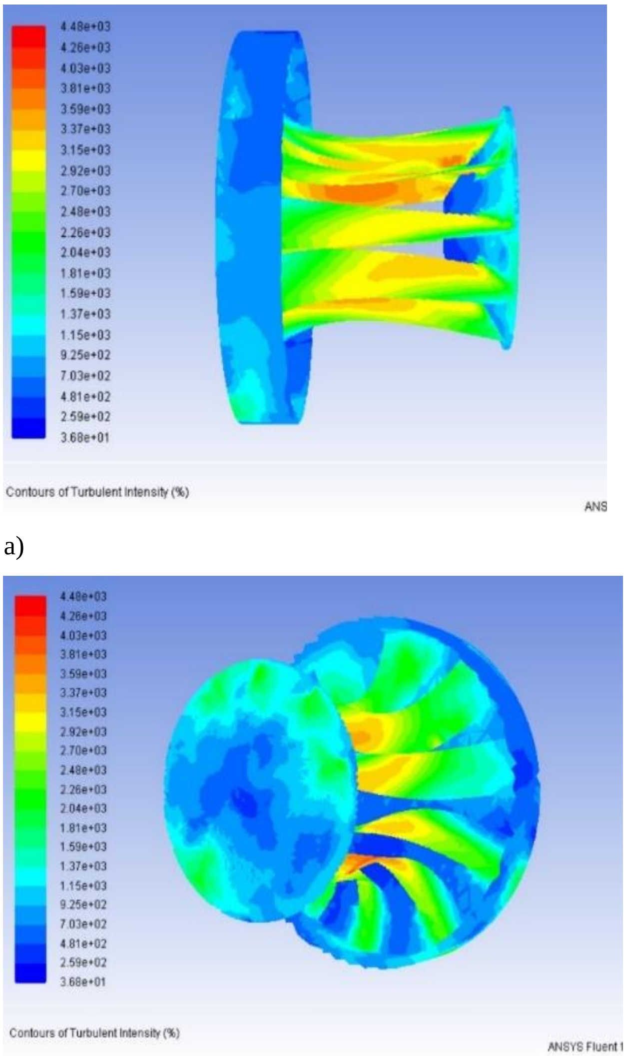

a)

b)

Fig. 18 Turbulent intensity contour in the turbine wheel

4.5 Contour of the Pressure at the Outlet of the Francis Turbine Wheel

The pressure variation observed in the Francis wheel presents areas of pressure drop. These pressure drop zones are the cause of instabilities in the turbine. the simulation made at the wheel outlet clearly shows us this pressure drop. the following figure shows the comparison of the pressure variation at the wheel outlet of our study and the study of (Jing & Liu, 2021) taken from the literature.

The comparison made between the Song loulou turbine and the turbine of (Jing & Liu 2021), shows us a low pressure zone which is localised by the presence of a cavitation vortex: this is the vortex. A high-pressure zone located on the edges of the turbine at the wheel outlet. The pressure difference at the various measurement points of the Francis de Songloulou turbine varies between 0 and 34800 Pa, whereas in the literature, the pressure difference at the various measurement points varies between 0 and 34200 Pa, i.e. a significant figure error rate evaluated at around 1.7%, which demonstrates the presence of centro-rotational vortices at the impeller outlet. These are characteristics of the pressure drop in the turbine wheel.

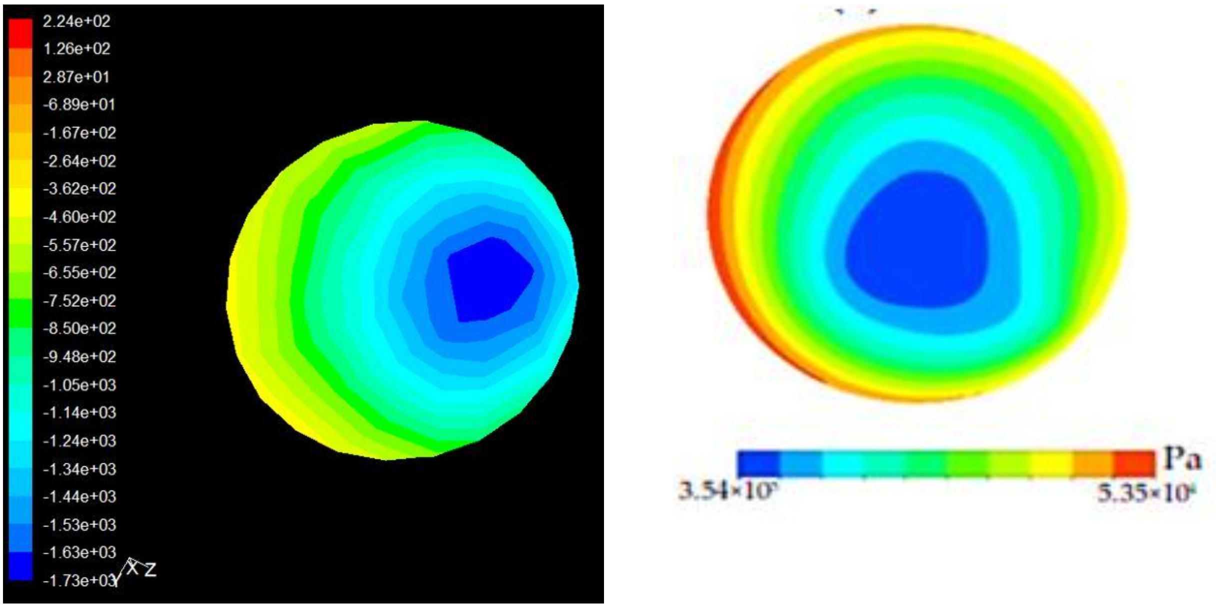

a) b)

Fig. 19 a) contour of pressure at the exit of the impeller from Song Loulou , b) contour of the pressure at the exit of the impeller (Jing & Liu, 2021).

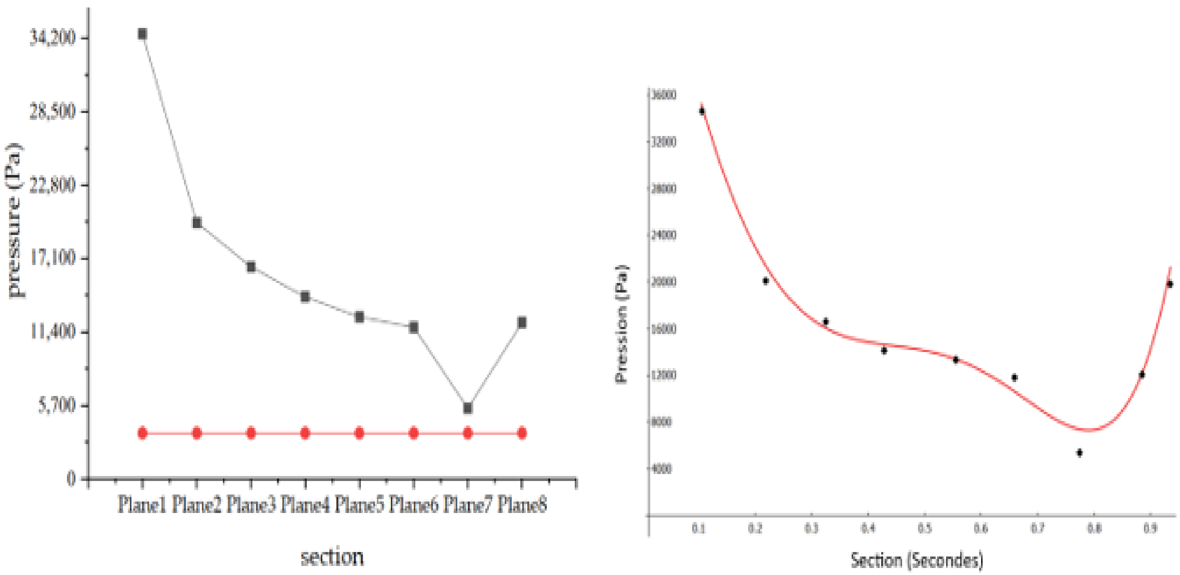

a) **b)**

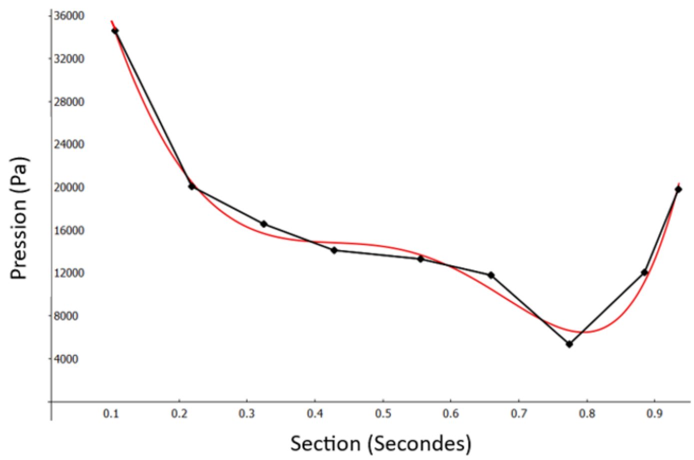

c)

Fig. 20 a) distribution de pression en sortie de roue de la turbine de (Jing & Liu, 2021) ; b) distribution de pression en sortie de roue de la turbine Francis de song loulou ; c) superposition of the two curves

5. CONCLUSION

In this article, CFD modeling was performed in the Francis turbine of the Song Loulou hydroelectric power station in order to know the behavior of the turbine in operation. The data of the boundary conditions allowed us to be in the same operating conditions. The results obtained allowed us to validate the working method by comparison with the work taken in the literature. First, we observed the uniformity of the flow in the spiral cover on the orthogonal, longitudinal and transverse plane; then the modeling done in the Francis wheel shows us the pressure variation; we clearly observed the areas of high pressure and the areas of low pressure localized to the upper surface of the blade, which indicates the presence of instabilities in the turbine. Finally, we evaluated this pressure variation at the wheel outlet and found that a cavitation flare forms in the Francis turbine of the Song Loulou hydroelectric power station. The results obtained were satisfactory insofar as the comparison with the works of the literature obtained practically the same pressure variations and the discovery of the presence of the cavitation flare which is a serious problem to be solved. The remainder of this article will attempt to resolve the cavitation phenomenon that has been observed.

CONFLICT OF INTEREST

The research team here works without funding in difficult conditions. it is clear that there is no financial conflict of interest to disclose. the aim is to make a significant contribution to science.

AUTHORS' CONTRIBUTION

Tientcheu-Nsiewe Maxwell is PhD lecturer at the School of Chemical Engineering and Mineral Industry, University of Ngaoundere, Cameroon, his contribution in this work is significant in the research of boundary conditions and modeling; **Denis Tcheukam-Toko**, is Professor and Head of Department at College of Technology, Department of Mechanical engineering, University of Buea, Cameroon. His guidance and advice add quality to the research team. **Bienvenu Kenmeugne** is a Professor at the Department of Mechanical engineering, National Higher School Polytechnics of the University of Yaoundé, Cameroon, **Alexis Kuitche**, Professor and Director of Academic Affairs, National School of Agro-Industrial Sciences, University of Ngaoundere, Cameroon; **Raoul Dieudonné Wafo**, PhD student and part-time lecturer at College of Technology, Department of Mechanical engineering, I am the principal author of this article.

REFERENCES

Alca, (2003). Analysis of the parietal pressure field of an angled turbine diffuser francis faculty of engineering sciences and techniques. Institute of Energy Sciences. https://doi.org/10.1088/1755-1315/15/6/062014.

Arn, C. (1998). *Analysis and prediction of the drop in efficiency of francis turbines by bubble cavitation*. Federal Institute of Technology in Lausanne. https://doi.org/10.5075/epfl-thesis-1799

Blommaert, G. (1995). Measurement of the unsteady velocity field at the exit of a Francis wheel with laser Doppler anemometry, *LMH-EPFL Lausanne*, https://www.researchgate.net/publication/37424169

Bousquet, Y., Binder, N., Roumeas, M., Dufour, G., Carbonneau, X., & Trébinjac, I. (2016) Numerical investigation of Kelvin- Helmholtz instability in a centrifugal compressor operating near stall. *Journal of Turbomachinery, 138* 071007-1: 9, https://doi.org/10.1115/1.4032457.

Bourdon, P. (2000). *Vibratory detection of cavitation erosion in Francis turbines*. PhD thesis https://doi.org/10.5075/epfl-thesis-2295

Ceccio, S., Gowing, S. & Gindroz B. (1995), A Comparaison of CSM bubble detection methods, pages 43, ASME https://api.semanticscholar.org/CorpusID:125999569

Ciocan, G., Mombelli, H., & Avellan, F. (2015). Francis turbine instabilities: Detailed scale model tests and measurements. *Resrarchgate*, 1-7. https://doi.org/1446629713.

Ding, N., T. Shigemitsu, I., Tomofumi, I. Takeru and I. Takuji (2021). Pressure fluctuation on casing wall and investigation to tip leakage flow of centro-rotating small hydro-turbine. *Proceedings of the Institution of Mechanical Engineers, Part A: Journal of Power and Energy*, *236*(3). https://doi.org/10.1177/09576509211052734

Duprat, C., Balarac, G., Metai, O. et al (2009). *Large-eddy simulation of draft tube flow and validation from experimental measurements*, Proceedings of the 3rd IAHR international meeting of the work group on cavitation and dynamic problems in hydraulic machinery and systems. https://www.researchgate.net/publication/341001609

Eric, O., & Elcilane, A. (2022, 3 November). de freitas, erb f. Lins, and Jerson R. p. go. 2020. Performance assessment of an indalma hydro-turbine. *Applied Sciences*, 1-13. https://doi.org/10.1007/s42452-020-03970-x

Gino, B (2000). *Study of the dynamic behavior of francis turbines: active control of their operating stability*. Federal Institute of Technology in Lausanne. https://doi.org/10.5075/epfl-thesis-2222

Gohil, R., & Saini. (2016). Numerical study of cavitation in francis turbine of a small hydro power plant. *Journal of Applied Fluid Mechanics*, *9*(1), 358-65. https://doi.org/10.18869/acadpub.jafm.68.224.24080

Gyanendra T., & Kumar, J. (2020). Utility of CFD in the design and performance analysis of hydraulic turbines a review. *Elsevier*, *462003*(211004), 2411-29. https://doi.org/10.1016/j.egyr.2020.09.004

Houde, S., Carrier, A., Buron, J. D., & Deschênes, C. (2014). Numerical analysis of a measured efficiency hysteresis on a bulb turbine model, *IOP Conf Ser Earth Environ Sci 22*:022009. https://doi.org/10.1088/1755-1315/22/2/022009

Jacob, J., & Married, D. (1988). Dynamic behavior of a Francis turbine at high load model-prototype comparisons. *LHB: Hydroscience Journal*, 3(4), 294-300. https://doi.org/10.1051/lhb/1988025

Jing, Y., & Liu, D. (2021). Pressure analysis in the draft tube of a pump-turbine under steady and transient conditions. *Energies*, *14*(4732), 1-13. https://doi.org/10.3390/en14164732

Khalfi, B. (2005). *Contribution to the development of a stress calculation code in a francis turbine*. Higher Technology School University of Quebec. https://doi.org/10.1016/j.advengsoft.2010.09.001

Maged, Y. (2003). Modeling of Vibratory Cavitation Erosion Test Results by a Weibull Distribution. *Journal of Testing and Evaluation*, *31*, 277-288. https://doi.org/10.1520/JTE12173J

Mauri, S. (2002). *Numerical Simulation and flow analysis of an elbow diffuser*. PhD thesis, EPFL No 2527, 2002 https://www.bing.com/ck/537ff9346c21

Max, K. (2014). *Numerical modelling of cavitation bubbles with the Finite Volume method*. https://doi.org/10.13140/RG.2.2.19259.46884.

Monica, S., Ciocan, G., & Avellan, F. (2009). *Analysis of the cavitating draft tube vortex in a francis turbine using particle image velocimetry measurements in two-phase flow*. *Journal of Fluids Engineering*, *130*(021105-1), 1-10. https://doi.org/10.1115/1.2813052

Nicolet, C., & Avellan, F. (2002). *New tools for the simulation of transient phenomena in francis turbine power plants*. Proceedings of The 21st Iahr Symposium On Hydraulic Machinery And Systems, Lausanne, Switzerland, *International Association For Hydraulic Research*. https://www.researchgate.net/publication/37467112

Pereira, F. (1997). *Prediction of cavitation erosion: Energetic approach*. Doctoral thesis, polytechnique fédérale of Lausanne. http://dx.doi.org/10.1115/1.2820729

Pellegrino, A. & Meskell, C. (2013) Vortex shedding from a wind turbine blade section at high angle of attack. *Journal of Wind Engineering and Industrial Aerodynamics*, *121*, 131–137 https://doi.org/10.1016/j.jweia.2013.08.002

Saeed, A., & Popov, V. (2012). Complete francis turbine flow simulation at derbendikan power station. *Advances in Fluid Mechanics*, *74*, 49-57. https://doi.org/10.2495/AFM120051

Wahidullah, H., & Vishnu, P. (2017). *Design and permance analysis of francis turbine for hydro power station on kunar river using cfd. International Journal of Advanced Research*, 1004-12. https://doi.org/10.21474/ijar01/4209.

Xavier, E., & Egusquiza, E. (2006). *Detection of cavitation in hydraulic turbines*. *Mechanical Systems and Signal Processing*, *20* (4), 983-1007. https://doi.org/10.1016/j.ymssp.2004.08.006.

Xiao, W., & Zongguo, Y. (2010). Numerical analysis of unsteady flow under high-head operating conditions in francis turbine. *Engineering Computations*, *27*(3), 365-86. https://doi.org/:10.1108/02644401011029934.

Zhumei, L., & Nie, C. (2022). *The effect of j-groove on vortex suppression and energy dissipation in a draft tube of francis turbine*. *Energies*, 1-20. https://doi.org/10.3390/en15051707.